

# Ionization State and Dielectric Constant in Cold Rarefied Hydrocarbon (CH) Plasmas of Inertial Confinement Fusion

A. Shvydky, A. V. Maximov, V. V. Karasiev, D. Haberberger, S. X. Hu, and V. N. Goncharov

Laboratory for Laser Energetics, University of Rochester

Inertial confinement fusion (ICF) has been an active field of research for more than 50 years because of its application as a future energy source. In laser-driven ICF, a cryogenically cooled, thin spherical shell of deuterium–tritium (DT) fuel is imploded and compressed by material ablation to form a high-density confinement around a central core where the conditions for thermonuclear ignition can be created. During the implosion, the ablation pressure launches multiple shocks through the DT shell and accelerates it inward. Later, the buildup of pressure in the compressing vapor region decelerates the shell and, at stagnation, creates the conditions in the central core closest to ignition. The pressure buildup and the temperature and density in the core at stagnation are strongly affected by the amount of material that is released from the shell into the vapor region during the implosion.

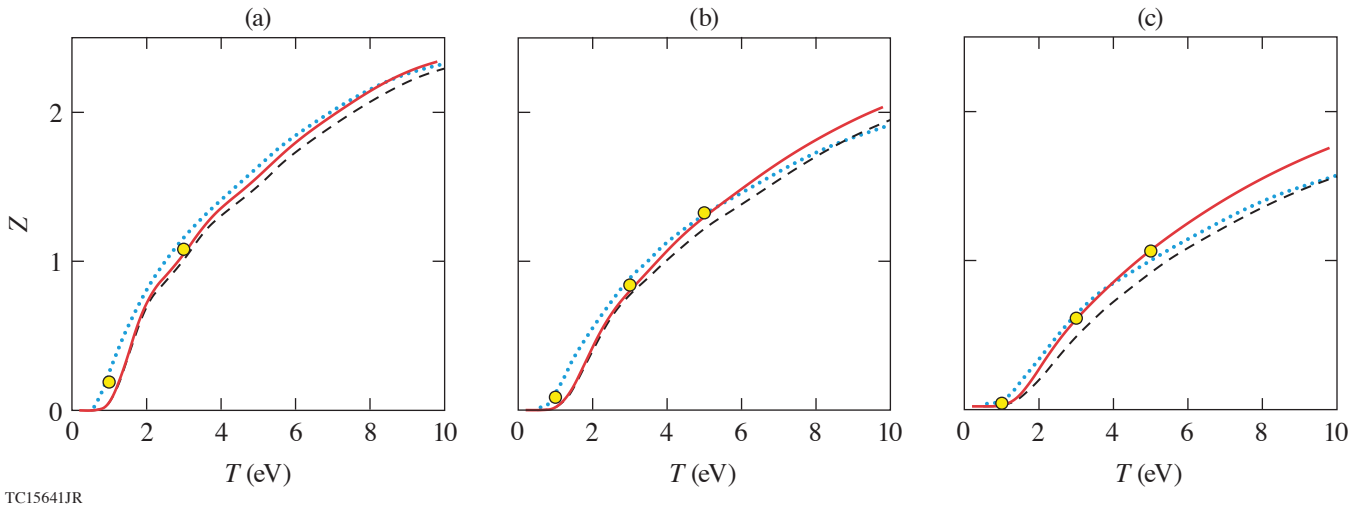
It is very challenging to measure the material released from the inner surface of the shell in the imploding capsule. However, in a planar geometry, one can access similar conditions with a CH foil and probe it using optical interferometry.<sup>1</sup> This technique was used for the first time in recent experiments<sup>2</sup> to diagnose the low-density part of the rarefaction wave formed when the shock driven by two OMEGA EP laser beams breaks out of a CH foil. The optical interferometry produces images in the focal plane that are proportional to the optical path (phase) that is accumulated by the wavefront of the probe laser propagating through the region of interest. The images are analyzed to obtain spatial profiles of the index of refraction. In low-density and low-temperature conditions, such as in the shock-release material, the plasma is partially ionized and the index of refraction is expected to have contributions from bound and free electrons and to depend on densities of atoms and free electrons which are connected to each other by the ionization state  $Z$ . Therefore, the index of refraction and  $Z$  are required to deduce the free-electron (plasma) density profiles from the interferograms.

The index of refraction at low densities and temperatures of shock-release material at a specific frequency of the laser probe is not generally expected to be available. While there are many studies of the optical properties of CH at solid or few times solid density,<sup>3</sup> no experimental data are available for rarefied CH gas at  $10^{-5}$  to  $10^{-2}$  g/cm<sup>3</sup> and few-eV temperatures. Recently *ab initio* simulations have become popular, are now accessible for calculating optical properties of arbitrary materials, and can be used to obtain the index of refraction at a desired laser frequency and thermodynamic conditions, i.e., mass density  $\rho$  and temperature  $T$ . The ionization state  $Z$  for CH material as a function of  $\rho$  and  $T$  is traditionally available via numerous  $Z$  tables used in ICF radiation-hydrodynamic codes. The simulations and analysis of the shock-release experiments<sup>2</sup> used the astrophysical opacity tables (AOT's) and collisional radiative equilibrium (CRE) tables, which predict different  $Z$ 's for the release conditions, and plasma index of refraction, which has no atomic contribution. These shortcomings motivated the present investigation.

In this summary we calculate the ionization state  $Z$  and the dielectric constant (which we use to obtain the index of refraction) as a function of density and temperature under conditions relevant to shock release. The conditions span several orders of magnitude in density  $\rho = 10^{-5}$  to  $10^{-2}$  g/cm<sup>3</sup> at a few-eV temperatures. We develop an algorithmically transparent, easy-to-follow method for calculating  $Z$  [which we call the Saha–Fermi–Debye–Hückel (SFDH) method] based on the free-energy minimization approach,<sup>4</sup> with free energy containing nonideal terms accounting for binary collisions and Coulomb interactions. We also obtain  $Z$  using *ab initio* calculations based on the Mermin–Kohn–Sham density functional theory (DFT) and test it against the semi-analytical method. After verifying the DFT-calculated ionization state against the semi-analytical method, we use the electron population

states obtained with the DFT and Kubo–Greenwood formulation to calculate the dielectric constant. Using the combined approach outlined above, we found that (a)  $Z$  calculated with the developed method and DFT agrees well with each other and is in reasonable agreement with that from CRE and AOT tables; (b) DFT-calculated atomic polarizabilities were within 20% of the reference data; and (c) a fit to the DFT-calculated dielectric constant contains an extra term due to atomic polarizabilities (i.e., contributions from bound states of electrons in atoms) that dominate the dielectric constant at low temperatures and  $Z$ . Based on these calculations, we revisited the shock-release experiments<sup>2</sup> and found more-accurate electron density profiles that, however, have not changed the main conclusions of Ref. 2.

Figure 1 shows the average ionization state  $Z$  as a function of temperature  $T$  for three mass densities  $\rho$ . The ionization state in Fig. 1 was obtained using four different sources: AOT tables, CRE tables, results of our SFDH method, and *ab initio* calculations. The *ab initio* calculations of  $Z$  used Kohn–Sham DFT and were performed using the Vienna *ab initio* simulation package (VASP) with the Perdew–Burke–Ernzerhof exchange–correlation (XC) functional. The DFT method calculates the electron states and their populations for each thermodynamic condition. Optical properties at each thermodynamic condition, which are used in the following sections, were calculated using the Kubo–Greenwood formulation<sup>5</sup> implemented in the KGEC@*Quantum Espresso*<sup>6</sup> package with the strongly constrained and appropriately normed XC functional.



TC15641JR

Figure 1

Average ionization state  $Z$  as a function of temperature from four different models: AOT (dashed black curves), CRE (dotted blue curves), our SFDH method (solid red curves), and the DFT calculations (yellow circles) for three mass densities: (a)  $10^{-4}$  g/cm<sup>3</sup>, (b)  $10^{-3}$  g/cm<sup>3</sup>, and (c)  $10^{-2}$  g/cm<sup>3</sup>.

As one can see from Fig. 1, the *ab initio* calculations (yellow circles) are in very good agreement with the calculations using the SFDH method (solid red curves) at 3- and 5-eV temperatures, while  $Z$  from AOT (dashed black curves) and CRE (dotted blue curves) are up to 20% off. At lower temperatures (1 eV), the DFT method predicts noticeably higher  $Z$  than SFDH. The discrepancy is caused by the self-interaction error inherent in the DFT local and semi-local approximations for the XC energy.<sup>7</sup> The electron self-interaction decreases the ionization energy of H and to a lesser degree C atoms and leads to an artificial increase in  $Z$ , which is more apparent for temperatures much smaller than the ionization energies.

Figure 2 shows the dependence of the dielectric constant of CH on the temperature for two densities at the OMEGA EP laser probe wavelength of  $\lambda = 263$  nm. Analysis of the index of refraction of CH at 1-, 3-, and 5-eV temperatures and 0.01- and 0.001-g/cm<sup>3</sup> densities leads to the following approximate formula for the real part of the dielectric constant (dashed red curves in Fig. 2):

$$\epsilon_{\text{DFT}} = 1 + 4\pi(1.7 \text{ \AA}^3 \cdot n_i - 4.9 \text{ \AA}^3 \cdot n_e), \quad (1)$$

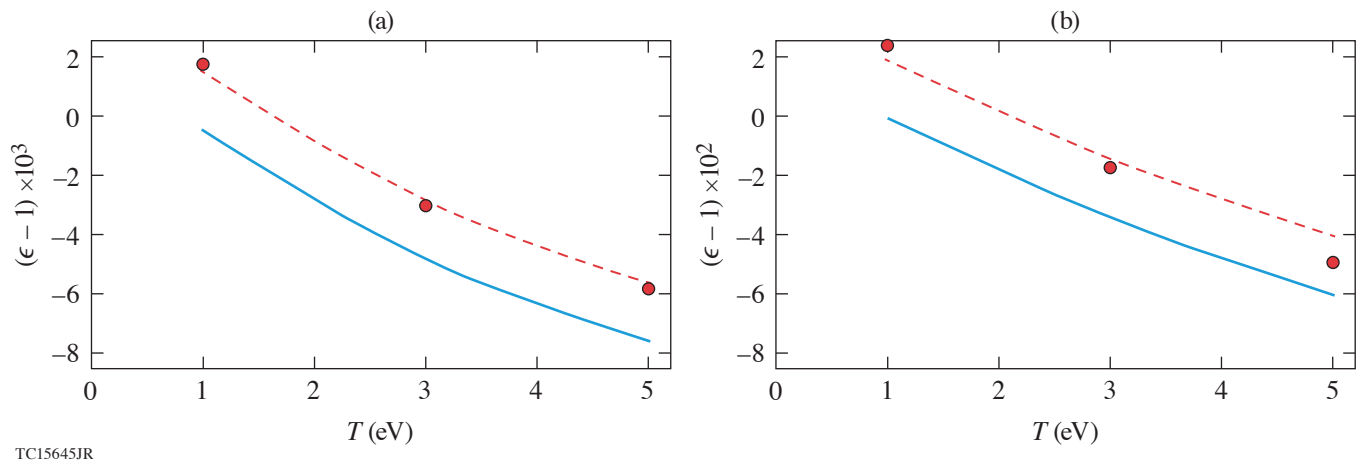


Figure 2

The real part of the dielectric permittivity in CH as a function of temperature from DFT calculations (red circles), from Eq. (1) (dashed red curves), and from Eq. (2) (solid blue curves) for mass densities of (a)  $10^{-3}$  g/cm<sup>3</sup> and (b)  $10^{-2}$  g/cm<sup>3</sup>.

where  $n_e = Z n_i$  is the electron density in  $\text{\AA}^{-3}$  and  $n_i$  is the ion density in  $\text{\AA}^{-3}$ ,  $n_i = \rho \langle A \rangle$ , where  $\langle A \rangle = 6.5$  amu is the average ion mass for 50% C – 50% H. The dielectric constant from Eq. (1) should be compared to the dielectric constant (solid blue curves in Fig. 2)

$$\epsilon_p = 1 - 4\pi \cdot 4.9 \text{\AA}^3 \cdot n_e \quad (2)$$

that was previously used in the analysis of the shock-release experiments.<sup>2</sup> The formula in Eq. (2) is the high-frequency plasma dielectric constant  $\epsilon_p = 1 - n_e/n_c$  (referred to below as the plasma dielectric constant),<sup>8</sup> where  $n_c$  is the critical density and  $n_c = 1/(4\pi \times 4.9) \text{\AA}^{-3}$  for  $\lambda = 263$  nm. The fit of Eq. (1) to the DFT-calculated dielectric constant contains a term  $\sim n_i$ , which is the contribution from atomic polarizabilities (i.e., the contribution from bound states of electrons in atoms) and is not present in the plasma dielectric constant [Eq. (2)].

The index of refraction calculated with the DFT method,  $n_{\text{DFT}} = \sqrt{\epsilon_{\text{DFT}}}$ , was used to revisit the interferometry data from the shock-release experiments.<sup>2</sup> Electron densities were found to be up to 40% higher and the position of the rarefaction wave up to 20  $\mu\text{m}$  further than reported in Ref. 2. It is important to note that for a laser drive of lower intensity than in Ref. 2, the plasma index of refraction is not valid and the DFT index of refraction must be used in the analysis of the shock-release experiments.

This material is based upon work supported by the Department of Energy National Nuclear Security Administration under Award Number DE-NA0003856, the University of Rochester, and the New York State Energy Research and Development Authority.

1. A. Howard *et al.*, Rev. Sci. Instrum. **89**, 10B107 (2018).
2. D. Haberberger *et al.*, Phys. Rev. Lett. **123**, 235001 (2019).
3. W. Theobald *et al.*, Phys. Plasmas **13**, 122702 (2006).
4. D. G. Hummer and D. Mihalas, Astrophys. J. **331**, 794 (1988).
5. R. Kubo, J. Phys. Soc. Jpn. **12**, 570 (1957); D. A. Greenwood, Proc. Phys. Soc. Lond. **71**, 585 (1958).
6. L. Calderín, V. V. Karasiev, and S. B. Trickey, Comput. Phys. Commun. **221**, 118 (2017); V. V. Karasiev, T. Sjoström, and S. B. Trickey, Comput. Phys. Commun. **185**, 3240 (2014).
7. J. P. Perdew and A. Zunger, Phys. Rev. B **23**, 5048 (1981).
8. J. D. Jackson, *Classical Electrodynamics*, 3rd ed. (Wiley, New York, 1999).